Pak. j. sci. ind. res. Ser. A: phys. sci. 2024 **67A**(3) 242-250

A DFT Investigation of Anion Photoelectron Spectroscopy and Franck Condon Spectroscopy of Cadmium Sulphide Clusters

Abdul Majid*, Mehreen Javed and Alia Jabeen*
Department of Physics, University of Gujrat, Gujrat, Pakistan

(received August 15, 2023; revised September 9, 2023; accepted December 21, 2023)

Abstract. This report involves density functional theory based study on CdS clusters to investigate electronic and vibronic properties of CdS and $(CdS)_2$ clusters in neutral and anionic forms keeping spin multiplicity into account. The symmetric CdS has one mode of vibration in infrared region (IR) but non-symmetric cluster $(CdS)_2$ exhibits six modes out of which three are active in IR region. The franck condon (FC) spectrum for (CdS) clusters exhibits the enhancement of FC factors by the increase in the number of atoms. The transformation from excited to ground state seems to be most likely and the most intense vibronic transition correspond to FC of 0.988 for CdS and 0.933 for $(CdS)_2$ cluster.

Keywords: cadmium sulfide (CdS), franck condon spectroscopy, franck condon (FC) factors, density functional theory

Introduction

By past few years, the fabrication and utilization in several applications of the nanosized cadmium sulphide (CdS) had been a hot area of research as well as for industrial interests (Firoozi and Hosseini-Sarvari, 2021; Shakoor *et al*., 2015). CdS is II-IV compound semiconductor that has been widely studied to investigate the novel structural, vibrational, optical as well as electrical properties for their implementations in optoelectronic and electronic devices. Despite the fact that the investigation of the materials ~1nm range is extremely proficient yet there are difficulties and complications with the experimental fabrications of ultrafine nano-particles (NPs) that tilt the balance in favour of utilizing the computational methods which provide the study of the material with any geometry and size. A large number of literature associated with the small clusters as well as nanoparticles of various compounds and elements are at hand (Berr *et al*., 2012; Fan *et al*., 2012; Pal *et al*., 2005). By considering the objectives, density functional theory (DFT) is privileged as it is a well known tool to maintain a balance in between efficiency and accuracy of that computations (Baerends and Gritsenko, 1997). The studies on II-VI materials have been performed by several groups by putting stress on its prototype CdS nanoparticles (NPs) and clusters. Gurin (Gurin, 1999; and 1996) investigated small-sized clusters of Zn_xS_y and Cd_xS_y (x, y=1-6) by utilizing semi- empirical computations. Nevertheless, later on they worked on the ab-initio technique to investigate the similar materials to discuss the constraints (e.g. geometry optimization) of semi-empirical techniques. Khabashesku carried out computations of infrared (IR) intensities along with the vibrational frequencies through the analysis of IR and vibrational spectra of silicene (Khabashesku *et al*., 1998). The structural properties (i.e. geometry of the system) along with electronic properties of wurtzite CdS surface were investigated using ab-initio methods (Rantala *et al*., 1998). A systematic study demonstrating electronic and optical characteristics of CdS/Te alloys can also be found in literature (Al-Douri *et al*., 2010).

Owing to increased knowledge on light matter interaction, several spectral analysis techniques have been developed during last couple of decades. Franck condon principle offers study of molecular vibronic spectrum to provide important information on the system (Huh *et al*., 2015). The extracted spectrum is employed to investigate structural and vibrational characteristics of various materials. Moreover, it provides information on the contribution of vibrational energy levels to electronic spectrum through the calculation of the intensity of vibronic transition . The value of Franck condon factor (FCF) is helpful to diagnose the electronic, vibrational, translation and rotational electronic energy levels that gives the insight into the structural, electronic and compositional properties of said material (Bullock, 2012; Thom, 2006). The franck condon (FC) spectroscopy gives an additional primacy over the charge state information that may not be offered by commonly used

*Author for correspondence;
E-mail: abdulmajid40@yahoo.com; aliajabeen777@gmail.com

spectroscopic techniques like IR and Raman. The rotational term parameters and spectroscopic constants for Bi_2 molecule were studied by computing the values of FCF by (Franklin and Perram, 1999). The capability of FC principle for spectroscopy have gained a lot of attention from many experts who evaluated electronic emission and absorption spectra for a number of compounds (Anthony *et al*., 2020; Zabuga *et al*., 2015). However, such work for CdS does not exist which may have restricted utilization of full potentials of the material.

The molecules become molecular anions on binding excess electrons and will more likely be stable if they do not go through the process of auto-detachment of electrons (Mooney *et al*., 2014). The electronic state of neutral molecules is energetically higher than ground state of anion. Employing this principle, anion-photo-electron-spectroscopy is an influential technique to explore electronic structure of molecules (Lu, 2021). Electrons are ejected upon shining light on anion molecules and electron number verses electronic K.E is recorded during such experiments (Simons, 2011). The photoelectron spectroscopy of CuO_2^- demonstrated photo-dissociation of $OCuO^-$ to produce $Cu^- + O_2$ (Mabbs *et al*., 2014). Though several compounds have been investigated using this technique but no relevant report is available on CdS clusters (Hang *et al*., 2015; Dreuw and Cederbaum, 2000; Mahapatra *et al*., 1999). A study on anion photoelectron spectroscopy of ZnO clusters using first principles method has been reported by this group. A combined study of franck condon analysis and photodetachement of anion provides very important information to understand molecules (Wang *et al*., 2020). Herein, we report anion-photoelectron-spectroscopy and franck condon spectroscopy of cadmium sulphide anions in the form of $(CdS)^{2-}$ or $(CdS)_2^{2-}$.

Computational details. The computations were carried out within DFT framework implemented ADF-molecule package (Te Velde *et al*., 2001) that works on the slater type orbitals. The ADF-module, provided with the graphical user interface (GUI), that simplifies the calculation of the electronic structure allowing its user to instinctively configure the simulation by the user-friendly environment (Jabeen *et al*., 2023; Majid *et al*., 2021; Majid *et al*., 2019a and b). The generalized gradient approximation (GGA) with B3LYP functional was employed (Fox, 2002) under basis sets of TZ2P for S and QZ4P for Cd atoms. The configurations were formed by utilizing the ADF (amsterdam density functional) by two atoms CdS monomer as well as four atoms $(CdS)_2$ dimmer clusters. The calculations were self consistent and the structures were geometrically optimized. The calculations were carried out to investigate various characteristics that includes molecular orbital theory (MOT)-structures, zero-point energy, iso-surfaces, frank condon spectrum and normal modes of vibration etc.

The frozen core approximation (Te Velde *et al*., 2001) was employed where Cd ($5s^2 4d^{10}$) and S ($3s^2 3p^4$) were considered as valence electronic states. ADF works on the basis on linear combination of atomic orbitals. The structures were optimized using numerical integration method (Wang *et al*., 2020). The $(CdS)_2$ is a diamond shape symmetrical and hence it has zero net dipole moment (Te Velde *et al*., 2001). Zero point energy at STP (standard temperature and pressure) was calculated using $E_{vb} = \sum_{k=1}^{3N-6} \left(U_k + \frac{1}{2}\right) h\nu_k$. (Sholl and Steckel, 2022). The important feature of this work is computation of vibronic intensities that was assisted with IR active modes of vibration. ADF package computes the force constant matrix in term of energy derivatives for different nuclear displacements during SCF cycle (Te Velde *et al*., 2001). The force constant matrix stands for force constant on similar footing as Slater type orbitals serves for atomic orbitals. Dipole moment is calculated by numerical integration method. The computational output helps to sketch vibrational spectra, MOT structures, iso-surfaces plots and franck condon spectrum.

We performed calculations for ground and anionic charge states of the clusters. First, the frequency calculations were analytically performed for ground state of molecule in the form $(CdS)_n$. Then same set of calculation was performed for the clusters in anionic state. In order to get the clusters anionic, a charge of 2- was introduced on them to obtain the structure in form of $(CdS)_n^{2-}$. The calculations were carried out considering spin multiplicity. For neutral $(CdS)_n$ being diamagnetic in nature, S=0 so multiplicity is 2(0)+1=1 indicating singlet state whereas in case of $(CdS)_n^{2-}$, considering all possibilities, for unpaired (paired) electrons having S=1(0) pointing to multiplicity 3(1) indicating triplet (singlet) state.

Results and Discussion

The calculated electronic and vibronic properties of CdS clusters are discussed in the following:

Structural parameters. In present work, the two different configurations are used as shown in Fig. 1(a &b). The

optimized structures are shown in Fig. 1. The first configuration utilized as CdS cluster possess Cs point group which incorporate the two symmetry elements E and σ therefore it contains the lower symmetry and reinforce the two irreducible depiction (A_1, A_2). The other configurations utilized as $(CdS)_2$ cluster possess the C_{2v} point group having symmetry elements of E, C_2, along with the $2\sigma_v$ and hence contributes towards the four irreducible representations A_1, A_2, B_1 and B_2. For the optimized structures of the clusters, the Cd–S bond lengths were found ranging between 0.2314–0.2613 nm which is close to the bond length for bulk wurtzite CdS (*i.e*: 0.2519 nm) structure. The bond angles for S-Cd-S and Cd-S-Cd were 75.6° and 104.2° respectively. The atoms in CdS structure are connected via double bond in the form of linear geometry and electron density is larger between them. On the other hand, the atoms in $(CdS)_2$ structure are connected via single bonds in the form of regular planar geometry of diamond shape (Shah *et al*., 2015; Rantala *et al*., 1996). The CdS clusters (Cs point group) possesses polar covalent bond along with the absence within the mirror symmetry, which arises due to the electronegativity difference of 0.89. This also leads to the fact that it has non-zero dipole moment equal to 16.172 D.

The MOT structures for CdS and $(CdS)_2$. The MOT structure for ground state CdS cluster is given in Fig. 2 whereas inset shows information about HOMO, LUMO and corresponding isosurfaces plots to reveal the contribution of atomic orbitals (AOs). The AO's $4d^{10}$ and $3s^2$ of Cd and S respectively combine to form filled un-restricted bonding б and anti-bonding б* MOs. The relatively higher energy AOs $5s^2$ and $3p^4$ of Cd and S contribute to form two bonding (б, π) and two of antibonding (б*, π*) MOs. The bonding MOs have lower energy than anti-bonding MOs which supports energy stabilization. Half of the difference of number of bonding and antibonding electrons gives bond order (6-0/2=3) that indicates that CdS is triply bonded with one б and two π MOs.

The HOMO with two spin paired electrons contains major contribution from $3p^4$ AO of S and its iso-surfaces diagram indicates attraction of electronic cloud towards S end of the structure. On the other hand, empty LUMO possesses equal share from $5s^2$ and $3p^4$ AOs of Cd and S atoms. LUMO gives the charge occupation probability in anionic state immediately higher in energy to HOMO and HOMO-LUMO gap is found equal to 21.96 meV. It is to be noted that iso-surfaces of LUMO have charge occupation probability in a plane perpendicular to HOMO plot. The average bond length for anion states is higher than neutral states of the clusters whereas triplet states revealed higher bond lengths when

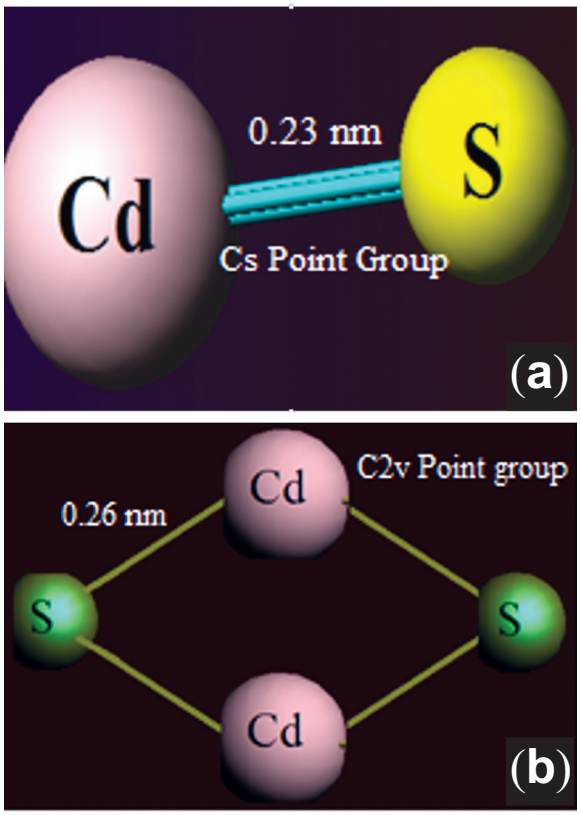

Fig. 1. The optimized structure of CdS clusters **(a)** 2-atoms **(b)** 4-atoms.

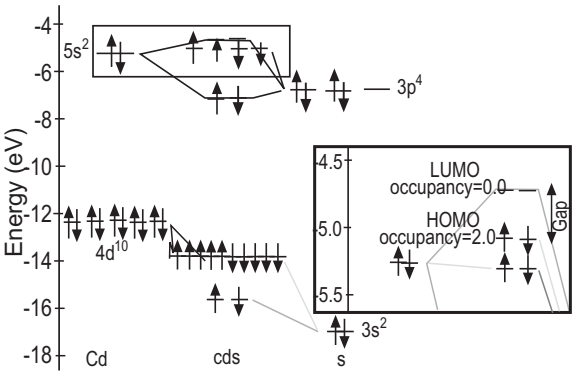

Fig. 2. The MOT structure for CdS cluster in ground state. The inset shows HOMO and LUMO levels.

compared with singlet states of same clusters. The value of bond energy is least for ground states regardless of spin multiplicity whereas triplet state has highest bond energy for all clusters. Similarly, HOMO-LUMO gap is highest for triplet states of the clusters. Table. 1. shows comparison of these values for ground and anionic states of clusters for all possible spin multiplicities.

The same set of calculations were performed for anionic state of CdS which shows contribution of $5s^2$ and $3p^4$ AO's of Cd and S to form HOMO and LUMO. The HOMO-LUMO gap is now 1.60 eV, which is greater than that of ground state depicting the electrons excitation to higher energy levels. The MOT structure for $(CdS)_2$ cluster in ground state and anionic states were also calculated to find locations and energy gaps between HOMO and LUMO. The main difference between the MOT structure in ground and anionic state is evident from energies of HOMO and LUMO that in anionic state energy levels shift upwards.

The iso-surfaces of CdS and $(CdS)_2$. The trend of charge spread in ground and anionic states for the clusters can be explored by analyzing the relevant iso-surfaces plots as shown in Fig. 3. LUMO and HOMO iso-surfaces point towards orbital type and bond information involved in the formation of clusters. The localization of charge density on Cd atoms indicates iconicity of bonds. The HOMO and LUMO are located on anions and cations respectively and closer look on HOMO points to lone pair configuration (Troparevsky and Chelikowsky, 2001). Due to lone pair type interaction, the bond length is observed to increase for two atoms cluster in order of CdS neutral < $(CdS)^{-2}$ singlet < $(CdS)^{-2}$ triplet and for four atoms cluster in order of $(CdS)_2$ neutral < $(CdS)_2^{-2}$ singlet < $(CdS)_2^{-2}$ triplet. The charge distribution reveals population at respective atoms of S and Cd to explain spatial charge within the clusters. The modified distribution of charge in anionic

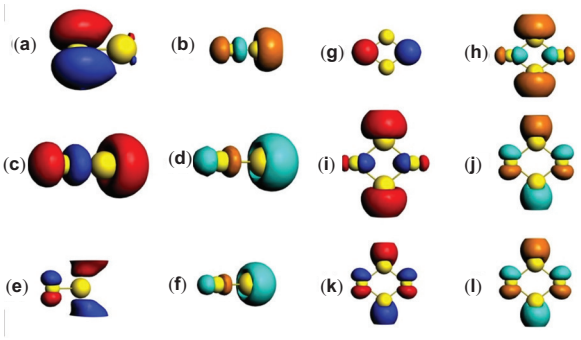

Fig. 3. Isosurface plots for **(a)** HOMO CdS **(b)** LUMO CdS **(c)** HOMO $(CdS)^{-2}$, singlet **(d)** LUMO $(CdS)^{-2}$, singlet **(e)** HOMO $(CdS)^{-2}$, triplet **(f)** LUMO $(CdS)^{-2}$

state points to different electric field so nuclei, which are slower in response to light interaction for being heavier than electron, rearrange themselves and produce a new nuclear configuration. After this, the rearrangement atoms adopt a new pattern of vibration which can be explored by analyzing the vibrational spectrum of CdS and $(CdS)_2$ cluster in ground and anionic states.

IR modes for CdS and $(CdS)_2$ clusters. IR vibrational spectra for CdS and $(CdS)_2$ clusters in ground and anionic states were calculated to investigate positions and intensities of active vibrational modes in IR region. These resonant modes of vibration can absorb photons of comparable frequency such that,

$$\text{Frequency}_{(\text{light absorbed})} = \text{Frequency(vibration)}$$

In contrast to the others modes, vibrational amplitude is a function of masses so heavier Cd moves less as compared to that of S which, being lighter, covers more distance away from equilibrium position. Keeping the condition of change in dipole moment into account, polar CdS has one active mode in IR region but non-polar $(CdS)_2$ cluster exhibits six modes as calculated

Table 1. Average bond length, bond energy, HOMO-LUMO gap and zero point energy of for CdS and $(CdS)_2$ clusters for different spin multiplicities

Cluster	Spin multiplicity	Average bond length (Å)	Bond energy (eV)	HOMO-LUMO gap (eV)	Zero-point energy (meV)
(CdS)	1	2.314	-2.099	0.245	21.96
$(CdS)^{-2}$	1	2.495	-1.445	1.606	16.03
$(CdS)^{-2}$	3	2.501	-0.674	1.764	16.00
$(CdS)^{-2}$	1	2.524	-7.385	1.048	77.47
$(CdS)_2^{-2}$	1	2.597	-7.388	0.671	60.10
$(CdS)_2^{-2}$	3	2.613	-7.107	1.977	66.16

by ADF interface and found in agreement with literature reviews (Hanes *et al*., 2023; Bandyopadhyay, 2009). The highly symmetric $(CdS)_2$ cluster has zero net change in dipole moment and hence due to lesser dipole strength it offers reduced IR optical activity. Therefore, only three modes of vibration are IR active, which by absorbing photons of comparable frequency; contribute to clear absorption bands in IR spectrum.

IR Spectra for CdS cluster in ground and anionic state. Figure 4 gives IR spectra for CdS in ground and anionic states. The absorption peak for ground vibrational state found at 176/cm exists in Far-IR region. The intra-molecular lattice vibration is an inherent molecular property and due to which atoms have never been locked and vibrate in a synchronized way around their mean positions. For this mode, the oscillator strength is $293.774x10^{-40}$ and absorption intensity is 13.009 km/mole. In anionic state of CdS, the peak is found at 257.164/cm in mid-IR region. The calculated values of dipole strength and absorption intensity of this mode are $622.925x10^{-40}esu^2cm^2$ and 40.154 km/ mole respectively.

IR spectra for $(CdS)_2$ cluster in ground and anionic state. In ground state $(CdS)_2$ cluster exhibits six modes with diverse intensities as shown in Fig. 5. Appearance of wideband instead of lines manifests the molecular nature of material. These modes are observed in far and mid IR region at frequencies 316.8/cm, 313.7/cm, 202.0/cm, 195.1/cm, 136.9/cm and 93.2/cm. Three modes are IR active and have prominent absorption intensities of 43.9, 21.6 and 12.6 (km/mole) supported by larger oscillator strengths whereas rest of three vibration modes are IR inactive as they have zero

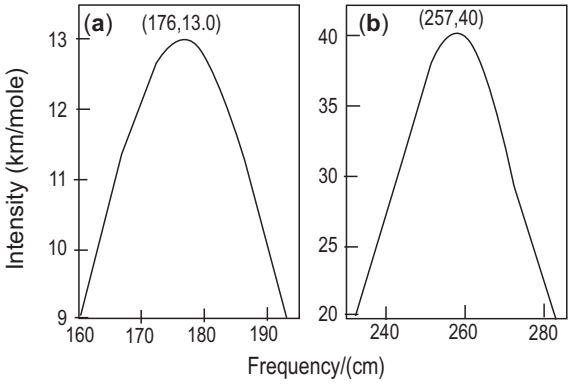

Fig. 4. The vibrational spectra for CdS clusters in **(a)** ground and **(b)** anionic state.

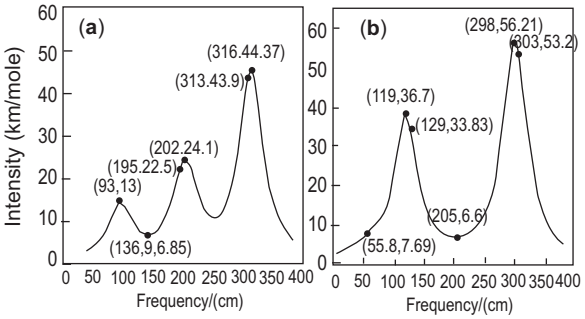

Fig. 5. IR spectrum for $(CdS)_2$ cluster **(a)** in ground state **(b)** in anionic state.

absorption intensity and very small dipole strength. Table. 2. shows detail of all these modes.

On the other hand, for the $(CdS)_2$ cluster in anionic state with singlet state, all six modes are observed in IR region out of which three modes with intensities of 56.2, 36.7 and 2.60 (km/mole) are IR active. In this work, symmetric stretching, scissoring and twisting modes are found IR inactive whereas asymmetric stretching, wagging and rocking are IR active. The comparison of the IR vibrational spectrum for ground and anionic states of structure indicate typical frequencies correspond to small or high values of optical absorption in CdS cluster. IR vibrational spectra of $(CdS)_2$ in ground and anionic state after absorbing a photon of resonant frequency with intensity of a particular IR active vibrational mode increased in anionic state as intensity of asymmetric stretching and rocking mode increases from 43.9 to 56.2 and 21.6 to 36.77 (km/mole) respectively.

Thermodynamic parameters. ADF uses laws of statistical mechanics to calculate the thermodynamic parameters including entropy, internal energy and heat capacity of molecules using translational, rotational, vibrational and electronic contributions. The calculation performed at room temperature and 1atm pressure for CdS and $(CdS)_2$ provided thermodynamic parameters given in Table. 2. The parameters for rotational and translational degrees of freedom remain unchanged for ground and anionic state however, for vibrational degree of freedom these parameters show small variation in anionic state which is due to increase in vibrational frequencies in anionic states.

It is obvious that entropy of system changes notably when compared with internal energy and heat capacity when number of atoms increases in molecules. Moreover,

Table 2. Thermodynamic parameters for CdS and $(CdS)_2$ clusters calculated for different multiplicities

Cluster	Spin multiplicity	Thermodynamic parameters	Translational	Rotational	Vibrational	Total
(CdS)	1	Entropy (cal/mole-K)	40.844	16.701	1.147	58.691
		Internal energy (Kcal/mole)	0.889	0.592	0.730	2.211
		Heat capacity (cal/mole-K)	2.981	1.987	1.566	6.534
$(CdS)^{-2}$	1	Entropy (cal/mole-K)	40.844	17.001	1.671	59.515
		Internal energy (Kcal/mole)	0.889	0.592	0.667	2.149
		Heat capacity (cal/mole-K)	2.981	1.987	1.748	6.716
$(CdS)^{-2}$	3	Entropy (cal/mole-K)	40.844	17.010	1.674	59.527
		Internal energy (Kcal/mole)	0.889	0.592	0.667	2.148
		Heat capacity (cal/mole-K)	2.981	1.987	1.749	6.717
$(CdS)_2$	1	Entropy (cal/mole-K)	42.910	27.122	13.448	83.480
		Internal energy (Kcal/mole)	0.889	0.889	3.891	5.668
		Heat capacity (cal/mole-K)	2.981	2.981	10.857	16.819
$(CdS)_2^{-2}$	1	Entropy (cal/mole-K)	42.910	27.464	16.397	86.771
		Internal energy (Kcal/mole)	0.889	0.889	3.765	5.542
		Heat capacity (cal/mole-K)	2.981	2.981	11.245	17.206
$(CdS)_2^{-2}$	3	Entropy (cal/mole-K)	42.910	27.483	16.670	87.063
		Internal energy (Kcal/mole)	0.889	0.889	3.830	5.607
		Heat capacity (cal/mole-K)	2.981	2.981	11.049	17.010

thermodynamic parameters are strongly affected for vibrational mode of freedom as compared to rotational and translational merely by changing the number of atoms.

The value of zero point energy level is spectroscopically important being more populated state at room temperature and according to Kasha's rule it involves most probable transitions. The values of zero point energy for CdS and $(CdS)_2$ cluster in ground state are 21.96 meV and 77.47 meV whereas in anionic state are 0.0159 eV and 0.0689 eV respectively. It is found that by increasing the number of atoms zero point energy level shifts to higher energy level as electrons in anionic states are at higher energy rather than in ground states. Zero point energy for singlet state is lower than corresponding value for ground states of the clusters.

Franck condon spectrum of clusters. Franck condon spectra were calculated for all clusters, however being lowest in energy the FC spectra of lowest multiplicity are shown in Fig. 6. A strong peak is observed which indicates the intensity of relevant vibronic transition. For CdS cluster, most intense vibronic transition occurs from zero energy level of the cluster in ground state to the zero energy level of the cluster in anionic state *i.e.*; 0-0 transition. Besides this most intense vibronic transition, several weak transitions are also observed and are listed in Table 3.

The franck condon spectrum for the CdS cluster is a good manifestation of energy quantization. Here two

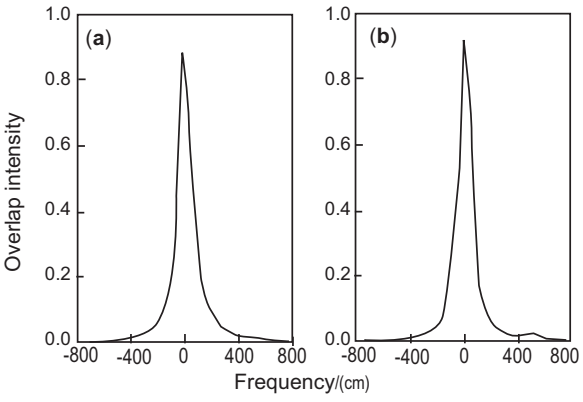

Fig. 6. FC spectrum for **(a)** CdS and **(b)** for $(CdS)_2$ neutral clusters.

Table 3. Overlap intensity as a function of frequency for CdS and $(CdS)_2$ clusters in ground state

	Frequency/cm)	Overlap intensity
CdS	0.000	0.983
	500.500	0.017
	1021.021	0.000
	1541.542	0.000
$(CdS)_2$	0.000	0.934
	100.100	0.029
	220.220	0.032
	460.460	0.002

prominent excitation peaks with diverse intensities depicts different degrees of vibrational wave functions overlap. It has 21 franck condon factors with value of 0-0 overlap integral as 0.991. Owing to large value of overlap integral, the maximum intensity of vibronic transition is 0.982. Moreover, the highly intense vibronic transition depicts the structural similarities between two states involved in the transition. The vibronic transitions for CdS are modeled in scaled Fig. 7.

It is a second class of vibronic spectra, involving a combination of electronic and vibronic structure. The dissociation threshold depicts that initial state is bound but final state is unbound for higher energy levels and have medium depth of potential well with only few vibrational energy levels. There exists limited but prominent vibrational structure but at higher energies transition span dissociates which leaves the spectrum unstructured.

Franck condon spectrum of $(CdS)_2$ cluster. The franck condon spectrum for $(CdS)_2$ clusters shown in Fig. 6 (b) indicates that the excitation peaks with diverse intensities reveal different degrees of vibrational wave functions overlap between ground and anionic vibrational energy levels (Shah *et al*., 2015). The vibronic transitions occur in IR, visible and ultraviolet regions declaring FCF spectrum a vibronic spectrum as combination of electronic transitions. The vibronic transitions for $(CdS)_2$ are modeled in scaled Fig. 8.

The franck condon factors are 230230 with ground-to-ground state overlap being equal to 0.933 that is responsible for most intense transition in the structure. Due to smaller 0-0 overlap integral, less intense vertical transitions are expected in $(CdS)_2$ than in CdS.

Conclusions

First principles calculations were performed to explore the electronic, vibrational and thermodynamic properties of CdS and $(CdS)_2$ keeping spin multiplicity into account. The bond energy for lowest spin multiplicity is lowest for the clusters. To probe the effect of anionic electronic state with charge of -2.0, we analyzed MOT structures by keeping into view HOMO-LUMO and their gap. Moreover, numerical results, electron densities and electrostatic potential using iso-surface plots are also included.

To grasp the vibrational transitions in CdS and $(CdS)_2$ the IR vibration spectra were analyzed. It was found that a symmetrical cluster CdS with non-zero dipole moment has an active mode in IR region whereas symmetrically structured $(CdS)_2$ cluster with zero dipole

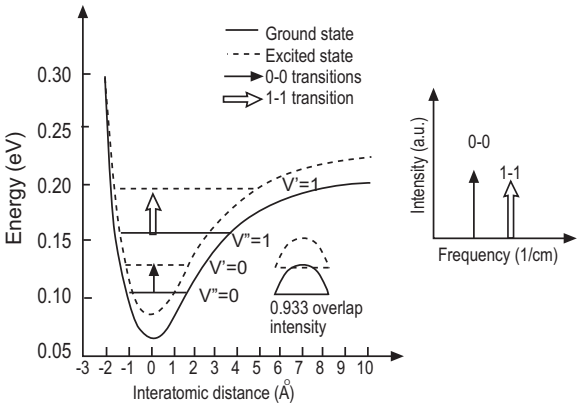

Fig. 7. Vibronic transitions for CdS extracted from franck condon spectrum.

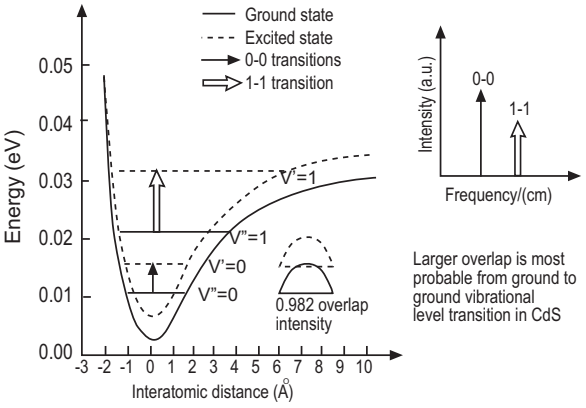

Fig. 8. Vibronic transitions for $(CdS)_2$ extracted from franck condon spectrum.

moment has six normal modes out of which three are IR active. It is concluded that asymmetric stretching, wagging and rocking are IR active modes of vibration, while symmetric stretching, twisting and scissoring are IR inactive.

The study of franck condon spectrum for CdS and $(CdS)_2$ clusters indicates that increases by the increase of number of atoms from two to four caused an increase in value of franck condon factor from 21 to 230230 which is decrease in overlap integral of 0.988 to 0.933 and increase in depth of related potential well. The 0-0 is the most probable and most intense vibronic transition for both structures.

Conflict of Interests. The authors declare that they have no conflicts of interest.

References

Al-Douri, Y., Reshak, A.H., Baaziz, H., Charifi, Z., Khenata, R., Ahmad, S., Hashim, U. 2010. An ab-initio study of the electronic structure and optical properties of CdS1- xTex alloys. *Solar Energy*, **84:** 1979-1984.

Anthony, E.J., Bolitho, E.M., Bridgewater, H.E., Carter, O.W., Donnelly, J.M., Imberti, C., Lant, E.C., Lermyte, F., Needham, R.J., Palau, M., Sadler, P.J., Shi, H., Wang, F., Zhang, W., Zhang, Z. 2020. Metallodrugs are unique: Opportunities and challenges of discovery and development. *Chemical Science*, **11:** pp.12888-12917.

Baerends, E.J., Gritsenko, O.V. 1997. A quantum chemical view of density functional theory. *The Journal of Physical Chemistry A,* **101:** 5383-5403.

Bandyopadhyay, D. 2009. Study of pure and doped hydrogenated germanium cages: a density functional investigation. *Nanotechnology*, **20:** 275202.

Berr, M.J., Schweinberger, F.F., Doblinger, M., Sanwald, K.E., Wolff, C., Breimeier, J., Crampton, A.S., Ridge, C.J., Tschurl, M., Heiz, U., Jackel, F., Feldmann, J. 2012. Size-selected subnanometer cluster catalysts on semiconductor nanocrystal films for atomic scale insight into photocatalysis. *Nano Letters*, **12:** pp.5903-5906.

Bullock, N.A. 2012. *Characterization of the LIBS Plasma of an Explosive Simulant, 3-Nitrobenzoic acid*: Arkansas State University. https://www.semanticscholar.org/paper/Characterization-of-the-LIBS-plasma-of-an-explosive-Bullock/ab174cf6e22ac06a8a12fdc6de2c17438f6699ce

Dreuw, A., Cederbaum, L. 2000. Tunnelling lifetimes of metastable and binding properties of stable covalent BeC n 2-(n= 4, 6) dianions. *The Journal of Chemical Physics*, **112:** 7400-7408.

Fan, J.A., Bao, K., Sun, L., Bao, J., Manoharan, V.N., Nordlander, P., Capasso, F. 2012. Plasmonic mode engineering with templated self-assembled nanoclusters. *Nano Letters*, **12:** 5318-5324.

Firoozi, S., Hosseini-Sarvari, M. 2021. Nanosized CdS as a reusable photocatalyst: the study of different reaction pathways between tertiary amines and aryl sulfonyl chlorides through visible-light-induced N-dealkylation and C–H activation processes. *The Journal of Organic Chemistry*, **86:** 2117-2134.

Fox, M., Bertsch, G.F. 2002. Optical properties of solids. *American Journal of Physics*, **12:** 1269-1270

Franklin, R.E., Perram, G.P. 1999. Laser excitation spectra and franck condon factors for Bi2X1Σ+ g→ A (0+ u). *Journal of Molecular Spectroscopy*, **194:** 1-7. https://www.sciencedirect.com/science/article/abs/pii/S0022285298977694

Gurin, V. 1996. Electronic structure of CdS cores in Cd thiolate complexes and clusters. *The Journal of Physical Chemistry*, **100:** 869-872. https://pubs.acs.org/doi/10.1021/j100020a066

Gurin, V. 1999. Quantum chemistry of quantum size-effects in semiconductors: Small clusters electronic structure calculations. *International Journal of Quantum Chemistry*, **71:** 337-341. onlinelibrary.wiley.com/doi/10.1002/%28SICI%291097-461X%281999%2971%3A4<337%3A%3AAID-QUA6>3.0.CO%3B2-Q

Hanes, A. T., Grieco, C., Lalisse, R. F., Hadad, C. M., Kohler, B. 2023. Vibrational relaxation by methylated xanthines in solution: Insights from 2D IR spectroscopy and calculations. *The Journal of Chemical Physics*, **158:** 044302.

Hang, T.D., Hung, H.M., Thiem, L.N., Nguyen, H.M.T. 2015. Electronic structure and thermochemical properties of neutral and anionic rhodium clusters Rhn, n= 2–13. evolution of structures and stabilities of binary clusters RhmM (M= Fe, Co, Ni; m= 1–6). *Computational and Theoretical Chemistry*, **1068:** 30-41.

Huh, J., Guerreschi, G.G., Peropadre, B., McClean, J.R., Aspuru-Guzik, A. 2015. Boson sampling for molecular vibronic spectra. *Nature Photonics*, **9:** 615-620.

Jabeen, A., Majid, A., Alkhedher, M., Haider, S., Akhtar, M. S. 2023. Impacts of structural downscaling of inorganic molecular crystals-A DFT study of Sb_2O_3. *Materials Science in Semiconductor Processing*,

166: 107729.

Khabashesku, V.N., Kudin, K.N., Margrave, J.L. 1998. Vibrational analysis of infrared spectra of matrix-isolated transient silenes on basis of density functional theory calculations. *Journal of Molecular Structure*, **443:** 175-189.

Kostjukova, L.O., Leontieva, S.V., Kostjukov, V.V. 2021. The vibronic absorption spectra and electronic states of proflavine in aqueous solution. *Computational and Theoretical Chemistry*, **1197:** 113144.

Lu, S.-J. 2021. Anion photoelectron spectroscopy and quantum chemistry calculations of TaSi 16-/0 clusters: global minimum fullerene-like cage structure, bonding and superatom properties. *New Journal of Chemistry*, **45:** 5266-5271. https://pubs.rsc.org/en/content/articlelanding/2021/nj/d1nj00214g#!

Mabbs, R., Holtgrewe, N., Dao, D.B., Lasinski, J. 2014. Photodetachment and photodissociation of the linear OCuO- molecular anion: energy and time dependence of Cu- production. *Physical Chemistry Chemical Physics*, **16:** 497-504. https://pubs.rsc.org/en/content/articlelanding/2014/cp/c3cp52986j#!

Mahapatra, S., Köppel, H., Cederbaum, L.S. 1999. Impact of nonadiabatic coupling between the conically intersecting X 2 A 1 and Ã 2 B 2 states of NO_2 on the negative ion photoelectron spectra of NO^-_2. *The Journal of Chemical Physics*, **110:** 5691-5701.

Majid, A., Zahid, S., Khan, S.U.D., Ahmad, A., Khan, S. 2021. Photoinjection and carrier recombination kinetics in photoanode based on (TM) FeO_3 adsorbed TiO_2 quantum dots. *Materials Science and Engineering: B*, **273:** 115423.

Majid, A., Jabeen, A., Khan, S.U.D., Haider, S. 2019b. Optical properties of titania–zirconia clusters: a TD-DFT study. *Journal of Cluster Science*, **30:** 707-713.

Majid, A., Jabeen, A., Khan, S.U.D., Haider, S. 2019a. First principles investigations of vibrational properties of titania and zirconia clusters. *Journal of Nanoparticle Research*, **21:** 1-15.

Mooney, C. R., Parkes, M. A., Zhang, L., Hailes, H. C., Simperler, A., Bearpark, M. J., Fielding, H. H. 2014. Competition between photodetachment and autodetachment of the 2 1 π π* state of the green fluorescent protein chromophore anion. *The Journal of Chemical Physics*, **140:** 205013. Parkes/0b 30f 41f2d26b0d824ebf745ea1b09816e9500e2

Pal, S., Goswami, B., Sarkar, P. 2005. Size-dependent properties of ZnmSn clusters: a density-functional tight-binding study. *The Journal of Chemical Physics*, **123:**

Rantala, T., Lantto, V., Rantala, T. 1998. Computational approaches to the chemical sensitivity of semiconducting tin dioxide. *Sensors and Actuators B: Chemical*, **47:** 59-64.

Rantala, T.T., Rantala, T.S., Lantto, V., Vaara, J. 1996. Surface relaxation of the (1010) face of wurtzite CdS. *Surface Science*, **352:** 77-82.

Shah, S.H., Azam, A., Rafiq, M.A. 2015. Atomistic simulations of CdS morphologies. *Crystal Growth & Design*, **15:** 1792-1800.

Shakoor, A., Hussain, F., Hassan, N., Majid, A., Bhatti, M.T., Siddique, H. 2015. A density functional theory study of Raman modes of cadmium hexathio hypodiphosphate (CdPS). *Materials Science-Poland*, **33:** 286-291.

Sholl, D.S., Steckel, J.A. 2022. *Density Functional Theory: A Practical Introduction*: 238pp. John Wiley & Sons., USA.

Simons, J. 2011. Theoretical study of negative molecular ions. *Annual Review of Physical Chemistry*, **62:** 107-28.

Te Velde, G.T., Bickelhaupt, F.M., Baerends, E.J., Fonseca, G.C., van Gisbergen, S.J., Snijders, J.G., Ziegler, T. 2001. Chemistry with ADF. *Journal of Computational Chemistry*, **22:** 931-967.

Thom, R.L. 2006. Spectroscopic investigations of intersystem crossing and triplet state structure in acetylene. *Ph.D. Thesis*, 97 pp., Massachusetts Institute of Technology. https://dspace.mit.edu/handle/1721.1/36261

Troparevsky, M. C., Chelikowsky, J. R. 2001. Structural and electronic properties of CdS and CdSe clusters. *The Journal of Chemical Physics*, **114:** 943-949.

Wang, J., Gao, Y., Kong, H., Kim, J., Choi, S., Ciucci, F., Hao, Y., Yang, S., Shao, Z., Lim, J., 2020. Non-precious-metal catalysts for alkaline water electrolysis: operando characterizations, theoretical calculations, and recent advances. *Chemical Society Reviews*, **49:** 9154-9196.

Zabuga, A.V., Kamrath, M.Z., Rizzo, T.R. 2015. Franck–Condon-like progressions in infrared spectra of biological molecules. *The Journal of Physical Chemistry A*, **119:** 10494-10501.